New Journal and we have not received input yet 19 (2021) 100176

Contents lists available at ScienceDirect

Computational Toxicology

journal homepage: www.sciencedirect.com/journal/computational-toxicology

Computational models reveal the potential of polycyclic aromatic hydrocarbons to inhibit aromatase, an important enzyme of the steroid biosynthesis pathway

Nikita Tiwari, Anjali Pandey, Ashutosh Kumar, Anil Mishra *

Department of Chemistry, University of Lucknow, Lucknow 226007, India

ARTICLE INFO

Edited by Mark Cronin

Keywords:
PAHs
Aromatase
DFT calculations
Mulliken charges
Docking

ABSTRACT

Polycyclic aromatic hydrocarbons (PAHs) are widespread toxic chemicals that may cause endocrine disruption via interaction with aromatase (CYP19A1) which is a vital enzyme of steroid biosynthesis pathway. Herein, we report the optimization of PAHs and oxy-PAHs employing density functional theory (DFT) with B3LYP/3-21G basis set to elucidate their frontier molecular orbitals, Mulliken charges as well as the chemical reactivity descriptors. The DFT outcome revealed that Indeno(1,2,3-cd)pyrene show the lowest HOMO-LUMO gap (3.42 Kcal/mol) as well as highest electrophilicity index and basicity. To assess the structure based inhibitory action of PAHs and their metabolites, these were docked into the active site cavity of CYP19A1. The docking simulation studies predicted that Indeno(1,2,3-cd)pyrene has the least binding energy (-10.76 Kcal/mol) which is in good agreement with the DFT calculations and might serve as a potent inhibitor to CYP19A1 comparable with its known inhibitor, exemestane which has binding affinity −11.73 Kcal/mol. The high binding affinity of oxy-PAHs was attributed to the presence of hydrogen bonds along with different hydrophobic interactions between the pollutant and the critical amino acids residues of the receptor. The results emphasized that PAHs can structurally mimic the binding pattern of exemestane to aromatase.

1. Introduction

In various tissues, elevated levels of androgens are often associated with serious health consequences, such as bone loss, polycystic ovary syndrome (PCOS), insulin resistance and diabetes, high cholesterol, high blood pressure and heart disease. In steroid biosynthesis pathway, androgens are aromatised to estrogens via action of important enzyme aromatase; also known as estrogen synthase. It is CYP19A1, a member of the cytochrome P450 superfamily, which are monooxygenases that catalyze many reactions involved in steroidogenesis. It is an important factor in sexual development. To maintain the basal androgen-estrogen ratio, aromatase, a cytochrome P450, catalyzes three consecutive hydroxylation reactions converting C19 androgens to aromatic C18 estrogenic steroids. Upon receiving electrons from NADPH-cytochrome P450 reductase, aromatase converts androstenedione and testosterone to estrone and estradiol, respectively [1] as shown in Fig. 1 [2]. CYP19A1 is involved in steroid biosynthesis and catalyzes the conversion of androgen to estrogen in mammalian tissues [3].

A number of environmental chemicals have been found to inhibit aromatase activity, resulting in a decrease in the level of estrogen or an increase in the level of androgen in cells. Several studies have reported that CYP19A1 is a critical enzyme for estrogen synthesis. As per the scoping review, polycyclic aromatic hydrocarbon compounds may act as antiestrogens and/or antiandrogens by directly binding with estrogen and androgen receptors [4]. For example, benz(a)anthracene, benzo(a)pyrene, fluoranthene, and chrysene were shown to inhibit androgenic activity [5]. Many of the hydroxylated PAHs metabolites have been detected in human urine [6]. It has been explained that benzo(a)pyrene induced infertility in the male reproductive system [7]. PAHs have an extensive body of literature describing their endocrine disruptive activity [8]. Although, numerous studies have shown that PAHs and their metabolites appear to impact aromatase [9], but the elucidation of the binding mode and important interactions of PAHs with CYP19A1 have not been reported yet. This study highlights the important interactions of PAHs and oxy-PAHs with human placental aromatase cytochrome P450 (CYP19A1) which eventually inhibit the CYP19A1 activity and leads to the accumulation of androgens. The crystal structure of CYP19A1 along with substrate analogue Androstenedione (ASD) (PDB

* Corresponding author.
E-mail address: nikitalko23@gmail.com (A. Mishra).

https://doi.org/10.1016/j.comtox.2021.100176
Received 19 February 2021; Received in revised form 3 May 2021; Accepted 16 June 2021
Available online 18 June 2021

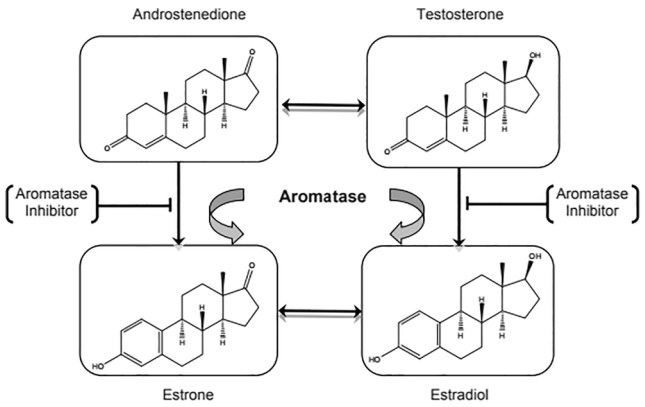

Fig. 1. Schematic diagram of the reaction catalyzed by aromatase enzyme.

ID: 3S79) is available. Exemestane, a known inhibitor of aromatase [10], binds in the active site of CYP19A1 and shows hydrogen bond interaction with Arg115 and Met374. Besides, many other xenobiotics had shown to inhibit the CYP19A1 such as PAHs to cause altered steroid biosynthesis [11].

In silico and virtual models offer a promising alternative to a better understanding of the effects of different chemicals on physiological processes and chemico-biological interactions. PAHs are one such group of diverse chemical entities which have received attention in the modern era of toxicology. Molecular docking and DFT studies were used to investigate the binding mode and stability of these PAHs and oxy-PAHs to human CYP19A1. Molecular docking studies facilitate the prediction of a possible molecular interaction of toxic ligands with enzymes of various pathways leading to the production of vital molecules and elucidate subsequent molecular cross-talk within the system [12]. In this study, nine common PAHs and few of their corresponding oxy-PAHs were used for the docking studies with CYP19A1 are: Indeno(1,2,3-cd) pyrene, Benzo(a)pyrene, Benzo(g,h,i)perylene, Benzo(a)anthracene, Chrysene, Pyrene, Anthracene, Phenanthrene, Fluorene, 2-hydroxyfluorene, 2-hydroxyphenanthrene, 2-hydroxyanthracene, 1-hydroxypyrene and 1-hydroxybenzo(a)pyrene. In order to find the molecular structure with the lowest energy, molecular orbitals, Mulliken charges and chemical reactivity parameters, DFT calculations were used. These parameters play an influential role in explaining the magnitude of pollutants interaction in the binding pocket of CYP19A1. The lowest HOMO-LUMO gap of the pollutant explains that HOMO of inhibitor may transfer its electrons to less energy, LUMO, of amino acids residues in the active site of an enzyme. These pollutants were chosen because they represent common PAHs sourced to petrogenic and pyrogenic emissions [13]. The results conclude that these PAHs can efficiently bind and can inhibit the activity of CYP19A1. Hence, the binding of PAHs with CYP19A1 affect the basal androgen to estrogen ratio which further affects the steroid biosynthesis pathway.

2. Materials and methods

2.1. DFT calculations

Quantum mechanical (QM) methods keep an important role for the calculation of molecular orbital properties [14]. In this investigation, QM calculation was implemented by using density functional theory (DFT) employing Becke's (B) [15] exchange functional combining Lee, Yang and Parr's (LYP) correlation functional [16] in Gaussian 09 program package for all pollutants [17]. Pople's 3-21G basis set was used to optimize the pollutants and for other calculations [18].

2.2. Molecular docking procedure

Computational docking studies were performed in order to assess the interaction of PAHs and oxy-PAHs with CYP19A1. AutoDock 4.2.6 [19] was used to perform the docking of PAHs and oxy-PAHs with CYP19A1. AutoDock utilizes a semi empirical free energy force field to calculate the binding free energy of a small molecule to a macromolecule. The coordinates of CYP19A1 were retrieved from the crystal structure of CYP19A1 bound to a substrate analogue Androstenedione (ASD) (PDB ID: 3S79) from the RCSB database. Receptor molecule was prepared by removing heteroatoms, also by adding explicit hydrogen molecules and associated Kollman charges (16.0) by utilizing the AutoDock Tools 1.5.6 and saved in .pdbqtfile format. Nine common PAHs and few of their corresponding oxy-PAHs used for the docking studies with CYP19A1 are: Indeno(1,2,3-cd)pyrene, Benzo(a)pyrene, Benzo(g,h,i)perylene, Benzo(a)anthracene, Chrysene, Pyrene, Anthracene, Phenanthrene, Fluorene, 2-hydroxyfluorene, 2-hydroxyphenanthrene, 2-hydroxyanthracene, 1-hydroxypyrene and 1-hydroxybenzo(a)pyrene. As a positive control, known inhibitor of CYP19A1, Exemestane was docked and compared with binding affinity scores of PAHs and their metabolites. The 3D structures of all the PAHs were drawn using Gauss View 5.0. The ligands were prepared by adding hydrogen atoms and Gasteiger charges and then saved in .pdbqt format. Ligand flexibility was used to specify the torsional degrees of freedom in ligand molecule. For docking purpose, Lamarckian genetic algorithm and grid supported energy evaluation method were adopted. The pose with the maximum binding affinity score and the corresponding interactions was selected and further visually inspected and analyzed in LigPlot.

3. Results and discussion

3.1. DFT calculation studies

The theoretical DFT calculations were performed with Gaussian09 software at B3LYP 3-21G basis set. The structural geometry was optimized by minimizing its energies compared to all geometrical variables without forcing any molecular symmetry restrictions. The molecular structure of the optimized pollutants (Fig. 2) was drawn by GaussView 5.0 [20].

3.1.1. Frontier molecular orbitals

Frontier molecular orbitals (FMOs) are the highest occupied molecular orbital (HOMO) with electrons, so it is an electron donor and the lowest unoccupied molecular orbital (LUMO) that has a space to accept electrons, so it is an electron acceptor. Both are very important quantum chemical parameters to calculate many important parameters such as the chemical reactivity descriptors. All the calculations are tabulated in Table 1. The isodensity surface plots of HOMO and LUMO for investigated pollutants are shown in Fig. 3.

In this study, Indeno(1,2,3-cd)pyrene amongst PAHs and 1-hydroxybenzo(a)pyrene amongst oxy-PAHs have the lowest HOMO-LUMO gap 3.42 eV and 3.31 eV respectively whereas Fluorene has the largest energy gap 5.18 eV. Large HOMO-LUMO gap related to high kinetic stability and low chemical reactivity and small HOMO-LUMO gap is important for low chemical stability, because addition of electrons to a high-lying LUMO and/ or removal of electrons from a low-lying HOMO is energetically favourable in any potential reaction.

3.1.2. Chemical reactivity descriptors

Hardness (η) and softness of all pollutantss were also calculated from the energies of frontier HOMOs and LUMOs considering Parr and Pearson interpretation [21,22] of DFT and Koopmans theorem [23]. The E_{HOMO} and E_{LUMO} are indicators for the prediction of the ionization potential ($I = -E_{HOMO}$) and the electron affinity ($A = -E_{LUMO}$) of molecules. Besides, the frontier molecular orbitals are used in estimation of other chemical reactivity descriptors such as electronegativity (χ),

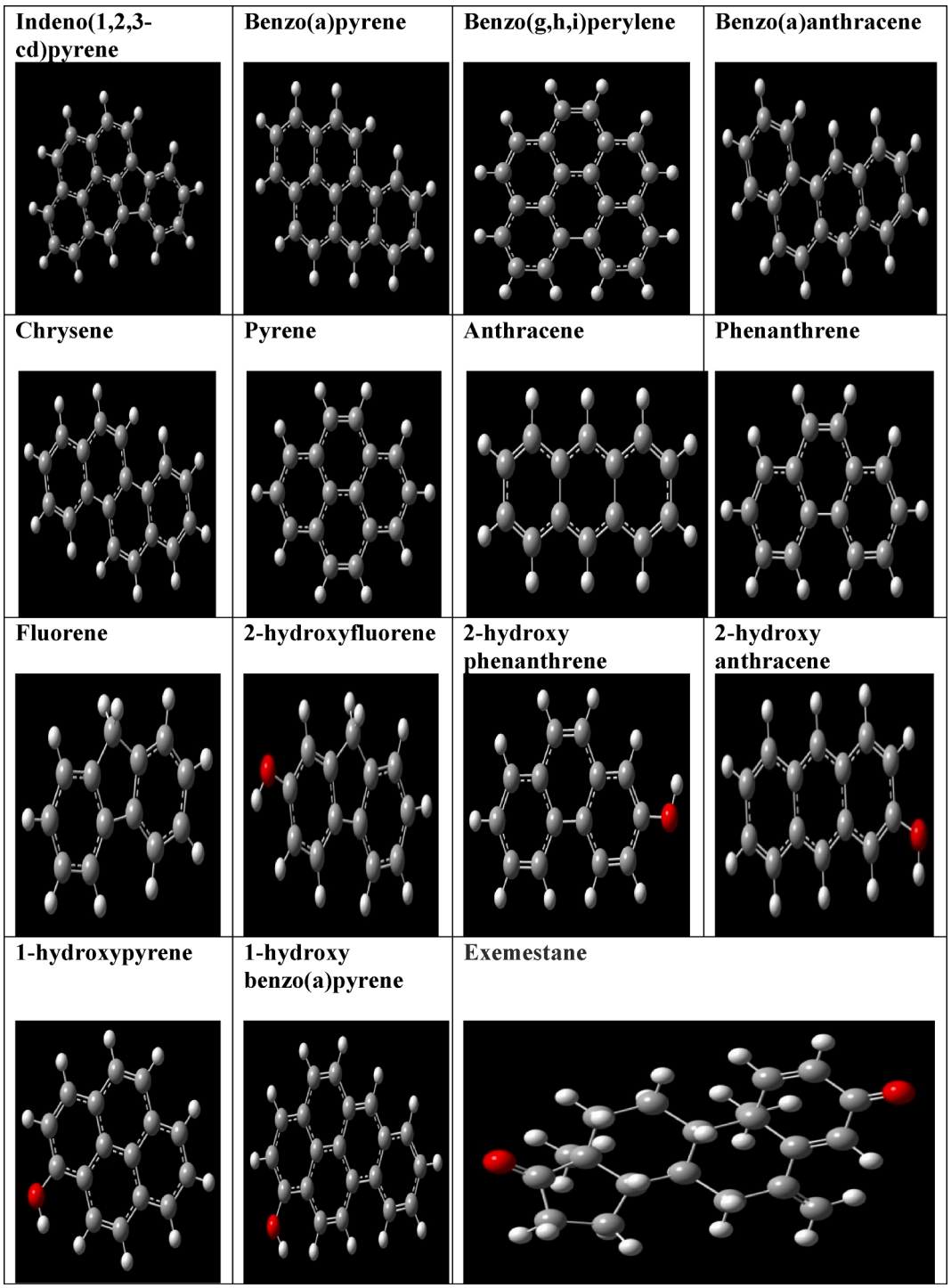

Fig. 2. Three dimensional representation of investigated pollutants and known inhibitor, exemestane.

global hardness (η), softness (δ), and electrophilicity (ω). The following equations are used for the calculation of chemical reactivity descriptors:

$$\chi = -1/2(E_{HOMO} + E_{LUMO})$$

$$\eta = -1/2(E_{HOMO} + E_{LUMO})$$

$$\delta = 1/\eta$$

$$\omega = \chi/2\eta$$

The χ value is a prediction of the power of the molecule to attract electrons i.e., Lewis acid, while small values of (χ) are indication of a good base. The global hardness (η) is a degree of their charge transfer prohibition; however, the global softness (δ) characterizes the ability of a molecule to accept electrons. Soft molecules are of a small energy gap between frontier molecular orbitals and are more reactive than the harder because they could easily transfer electrons to the acceptors. The electrophilicity (ω), calculated from the electronegativity and chemical hardness, is an indicator of lower energy difference due to the highest electron movement between the acceptor, LUMO, and the donor, HOMO. Amongst other PAHs, Indeno(1,2,3-cd)pyrene showed high basicity ($\chi = 3.78$) and high electrophilicity index ($\omega = 4.17$).

Table 1
Calculated electronegativity (χ), global hardness (η), softness (δ), global electrophilicity index (ω), the ionization potential (I) and the electron affinity (A) (in eV) of investigated pollutants.

Compound	HOMO	LUMO	ΔE	χ	η	δ	ω	I	A
Exemestane	−6.23	−1.61	4.62	3.92	2.31	0.43	3.32	6.23	1.61
Indeno(1,2,3-cd)pyrene	−5.49	−2.07	3.42	3.78	1.71	0.58	4.17	5.49	2.07
Benzo(a)pyrene	−5.24	−1.79	3.45	3.51	1.72	0.58	3.58	5.24	1.79
Benzo(g,h,i)perylene	−5.35	−1.72	3.63	3.53	1.81	0.55	3.44	5.35	1.72
Benzo(a)anthracene	−5.45	−1.58	3.87	3.51	1.93	0.51	3.19	5.45	1.58
Chrysene	−5.65	−1.30	4.35	3.47	2.17	0.46	2.77	5.65	1.30
Pyrene	−5.45	−1.53	3.92	3.49	1.96	0.51	3.10	5.45	1.53
Anthracene	−5.34	−1.65	3.69	3.49	1.84	0.54	3.30	5.34	1.65
Phenanthrene	−5.87	−1.01	4.86	3.44	2.43	0.41	2.43	5.87	1.01
Fluorene	−5.89	−0.71	5.18	3.30	2.59	0.38	2.10	5.89	0.71
2-hydroxyfluorene	−5.45	−0.53	4.92	2.99	2.46	0.40	1.81	5.45	0.53
2-hydroxyphenanthrene	−5.72	−1.02	4.70	3.37	2.35	0.42	2.41	5.72	1.02
2-hydroxyanthracene	−5.21	−1.57	3.64	3.39	1.82	0.54	3.15	5.21	1.57
1-hydroxypyrene	−5.19	−1.44	3.75	3.31	1.87	0.53	2.92	5.19	1.44
1-hydroxy benzo(a)pyrene	−5.03	−1.72	3.31	3.37	1.65	0.60	3.44	5.03	1.72

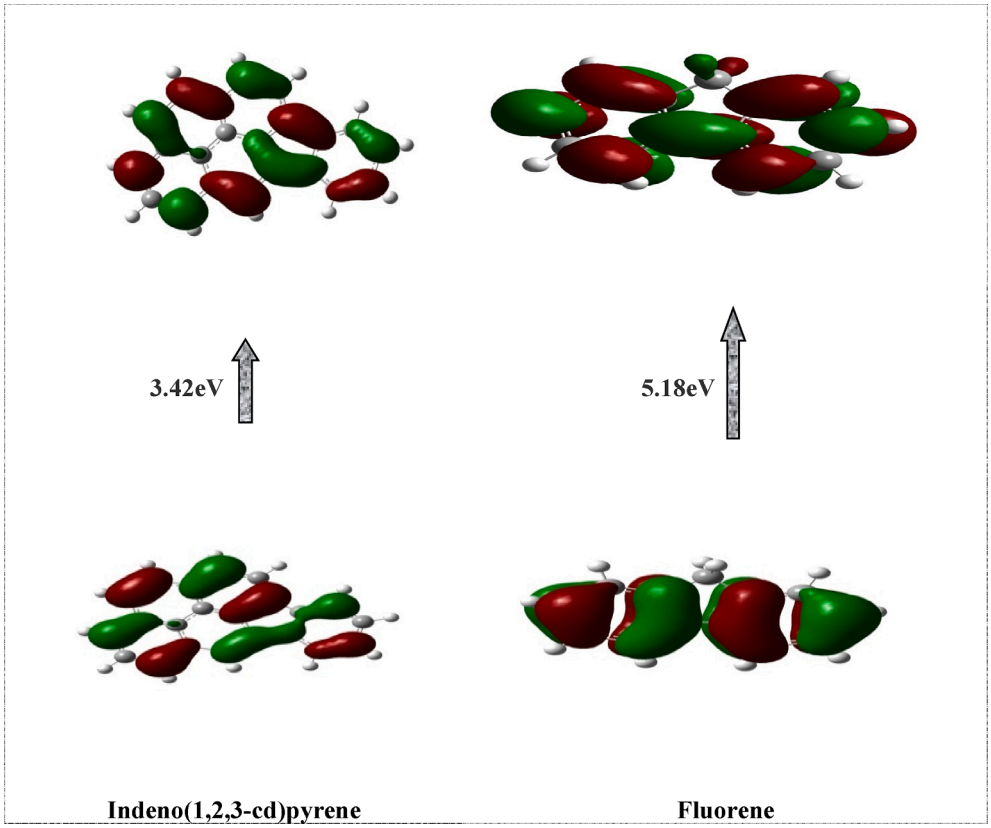

Fig. 3. The calculated ground state isodensity surface plots for Frontier molecular orbitals (FMOs) for investigated pollutants.

3.1.3. Mulliken atomic charges

The Mulliken atomic charges of the estimated pollutants were calculated by the DFT using B3LYP as a method at 3-21G basis set, the data for all the five oxy-PAHs were tabulated in Table 2. It showed that the C11 is the most positive and O1 have the most negative charge for 2-hydroxyfluorene. On the other hand, it is observed that the most nucleophilic center of 2-hydroxyphenanthrene is O1 which is the most electrophilic susceptibility position. However, O23, O1 and O32 are the most negative charges of 2-hydroxyanthracene, 1-hydroxypyrene and 1-hydroxybenzo(a)pyrene respectively. The positively charged centers are the most susceptible sites for nucleophilic attacks. However, the most negatively charged centers are the most susceptible sites for electrophilic one.

3.2. Molecular docking

Molecular docking is an extensively used computational approach to validate the binding of the suitable orientation of small molecule with the receptor protein. Results of this study revealed that due to the structural similarity of the benzene rings of PAHs with known inhibitor, exemestane, they are expected to mimic the binding mode at the active site of CYP19A1. PAHs and oxy-PAHs have a binding energy in the range of − 7.30 to − 10.76 kcal/mol which is comparable to exemestane (−11.73 kcal/mol) as shown in Table 3. These pollutants occupied the active site cavity comprising of residues such as Arg115, Ile133, Phe134, Asp309, Val370, Leu372, Val373, Met374, Leu477 and Ser478, in the same manner as that of exemestane as shown in Fig. 4. Except ordinary hydrogen bonding, nonbonding interactions are frequently used term to

Table 2
The Mulliken atomic charges of the five estimated oxy-PAHs.

2-hydroxy fluorene		2-hydroxy phenanthrene		2-hydroxy anthracene		1-hydroxy pyrene		1-hydroxy benzo(a)pyrene	
1O	−0.602706	1O	−0.602352	1C	0.005	1O	−0.603240	1C	−0.014652
2C	−0.483393	2C	−0.014840	2C	−0.000873	2C	−0.012254	2C	−0.011887
3C	0.049	3C	−0.007138	3C	0.005	3C	−0.010217	3C	−0.016316
4C	0.048	4C	−0.005242	4C	1E-05	4C	−0.004297	4C	0.009
5C	0.032	5C	−0.008013	5C	−0.202198	5C	−0.005183	5C	−0.012527
6C	0.042	6C	−0.181140	6C	−0.196166	6C	−0.000663	6C	−0.001137
7C	−0.227079	7C	−0.177396	7C	−0.219417	7C	0.001	7C	−0.003888
8C	−0.222173	8C	−0.192844	8C	−0.183258	8C	−0.191411	8C	0.003
9C	−0.225728	9C	−0.192098	9C	−0.182449	9C	−0.171121	9C	−0.197810
10C	−0.223915	10C	−0.218148	10C	−0.180728	10C	−0.176751	10C	−0.176310
11C	0.295	11C	−0.183792	11C	0.288	11C	−0.182193	11C	−0.179400
12C	−0.211748	12C	0.291	12C	−0.174897	12C	0.26	12C	−0.188238
13C	−0.182771	13C	−0.173345	13C	−0.185096	13C	−0.193444	13C	−0.175887
14C	−0.180278	14C	−0.179739	14C	−0.187596	14C	−0.194065	14C	0.263
		15C	−0.184533	15C	−0.600518	15C	−0.192030	15C	−0.195026
				23O		16C	−0.165389	16C	−0.187916
						17C	−0.176655	17C	−0.180115
								18C	−0.166482
								19C	−0.181072
								20C	−0.183579
								32O	−0.603143

Table 3
Details of molecular docking results: the summary of binding affinities (kcal/mol) and the H-bond or hydrogen bond as well as hydrophobic interactions of the PAHs-CYP19A1 complexes.

Compound	Binding Energy (kcal/mol)	Type of interactions		Number of bonds		Common Residues
		H-bond residues	Hydrophobic bond residues	H-Bonds	Hydrophobic Bonds	
Exemestane	−11.73	Arg115 (2.88 Å), Met374 (2.99 Å)	Val373, Ala306, Thr310, Trp224, Asp309, Ser478, Leu477, Val370, Leu372, Phe134, Ile133	2	11	**100%**
Indeno(1,2,3-cd) pyrene	−10.76	–	Arg115, Met374, Val373, Ala306, Thr310, Phe221, Asp309, Ser478, Leu477, Val370, Leu372, Ile133	0	12	**85%**
Benzo(a) pyrene	−10.07	–	Arg115, Met374, Val373, Ala306, Thr310, Leu477, Leu372, Ile133	0	8	**62%**
Benzo(g,h,i) perylene	−9.86	–	Arg115, Ala306, Thr310, Phe221, Trp224, Asp309, Ser478, Leu477, Leu372, Ile133	0	10	**69%**
Benzo(a) anthracene	−9.69	–	Arg115, Met374, Val373, Ala306, Thr310, Trp224, Leu477, Leu372, Phe134	0	9	**69%**
Chrysene	−9.35	–	Arg115, Met374, Val373, Ala306, Thr310, Trp224, Asp309, Leu477, Leu372, Ile133	0	10	**77%**
Pyrene	−8.34	–	Arg115, Met374, Val370, Thr310, Leu477, Leu372, Ile133, Phe134	0	8	**62%**
Anthracene	−7.87	–	Arg115, Val370, Thr310, Leu372, Ile133, Phe134	0	6	**46%**
Phenanthrene	−7.43	–	Ala306, Thr310, Trp224	0	3	**23%**
Fluorene	−7.30	–	Arg115, Ala306, Val370, Thr310, Ile133, Phe134	0	6	**46%**
2-hydroxy fluorene	−7.46	Leu372 (3.15 Å)	Val373, Ala306, Thr310, Val370, Phe134, Ile133	1	6	**54%**
2-hydroxy phenanthrene	−7.69	Ala306 (2.94 Å), Thr310 (3.05 Å)	Arg115, Trp224, Leu477, Phe134, Ile133	2	5	**54%**
2-hydroxy anthracene	−8.03	Leu372 (2.90 Å), Met374 (3.06 Å)	Arg115, Val373, Ala306, Thr310, Val370, Phe134, Ile133	2	7	**69%**
1-hydroxy pyrene	−8.60	Arg115 (2.96 Å), Met374 (2.90 Å)	Thr310, Leu477, Leu372, Phe134, Ile133	2	5	**54%**
1-hydroxy benzo(a) pyrene	−10.15	Arg115 (2.89 Å), Met374 (2.91 Å)	Ala306, Thr310, Leu477, Leu372, Phe134, Ile133	2	6	**62%**

determine the shape and behavior of molecules. These results suggest that all the studied pollutants can efficiently bind in the active site of CYP19A1. Moreover, Indeno(1,2,3-cd)pyrene along with oxy-PAHs seems to be the potent inhibitor for CYP19A1. Hence, inhibition of CYP19A1 by PAHs and oxy-PAHs can disbalance the basal ratio of androgen-estrogen in the steroid biosynthesis pathway.

As previously discussed from the DFT calculations, the negative Mulliken charges on oxygen atoms in oxy-PAHs could be used for hydrogen bond interactions with protein receptors. The energy levels of HOMOs are between −5.03 eV to −5.89 eV; however, the LUMOs are in between −0.53 eV to −2.07 eV depending on the conjugation as well as the presence of polar groups. Moreover, low FMO energy gap ($\Delta E = 3.42$), high basicity ($\chi = 3.78$) and high electrophilicity index ($\omega = 4.17$) of Indeno(1,2,3-cd)pyrene compared to others could be another effect on the binding affinity. Also, docking results showed that Indeno(1,2,3-cd)pyrene binds to aromatase with least binding energy (-10.76 kcal/mol) thus, complimenting the DFT studies. All these factors could share together with different extent to significantly impact the degree of the binding affinity of these pollutants with the active protein sites.

4. Conclusion

In steroid biosynthesis pathway, aromatase catalyzes the last steps of estrogen biosynthesis from androgens. The inhibition of CYP19A1

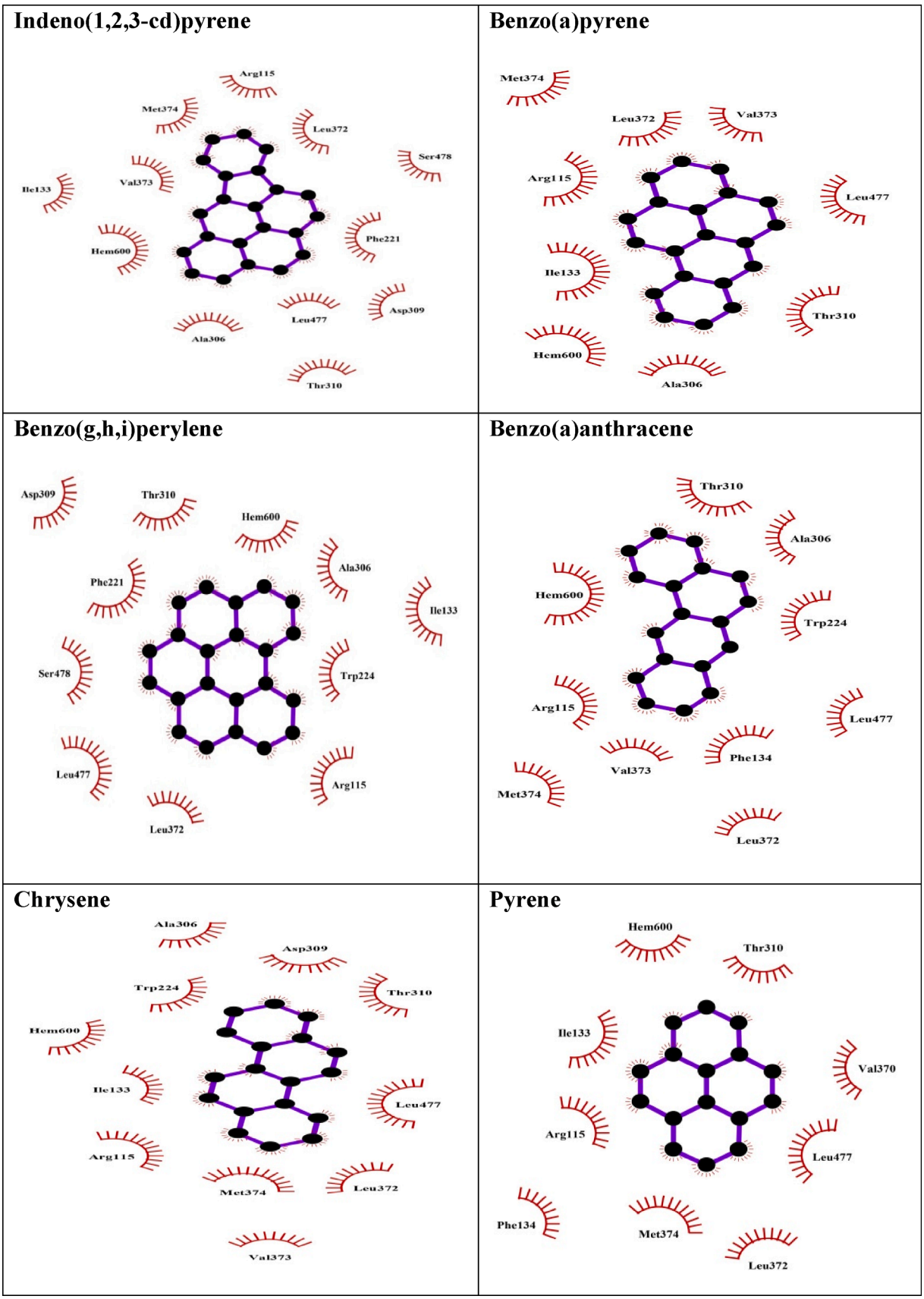

Fig. 4. The binding interaction of PAHs and oxy-PAHs with CYP19A1. The interacting residues of CYP19A1 residues are represented in red semi-circle form and the green dotted line shows the hydrogen bond interactions. (For interpretation of the references to colour in this figure legend, the reader is referred to the web version of this article.)

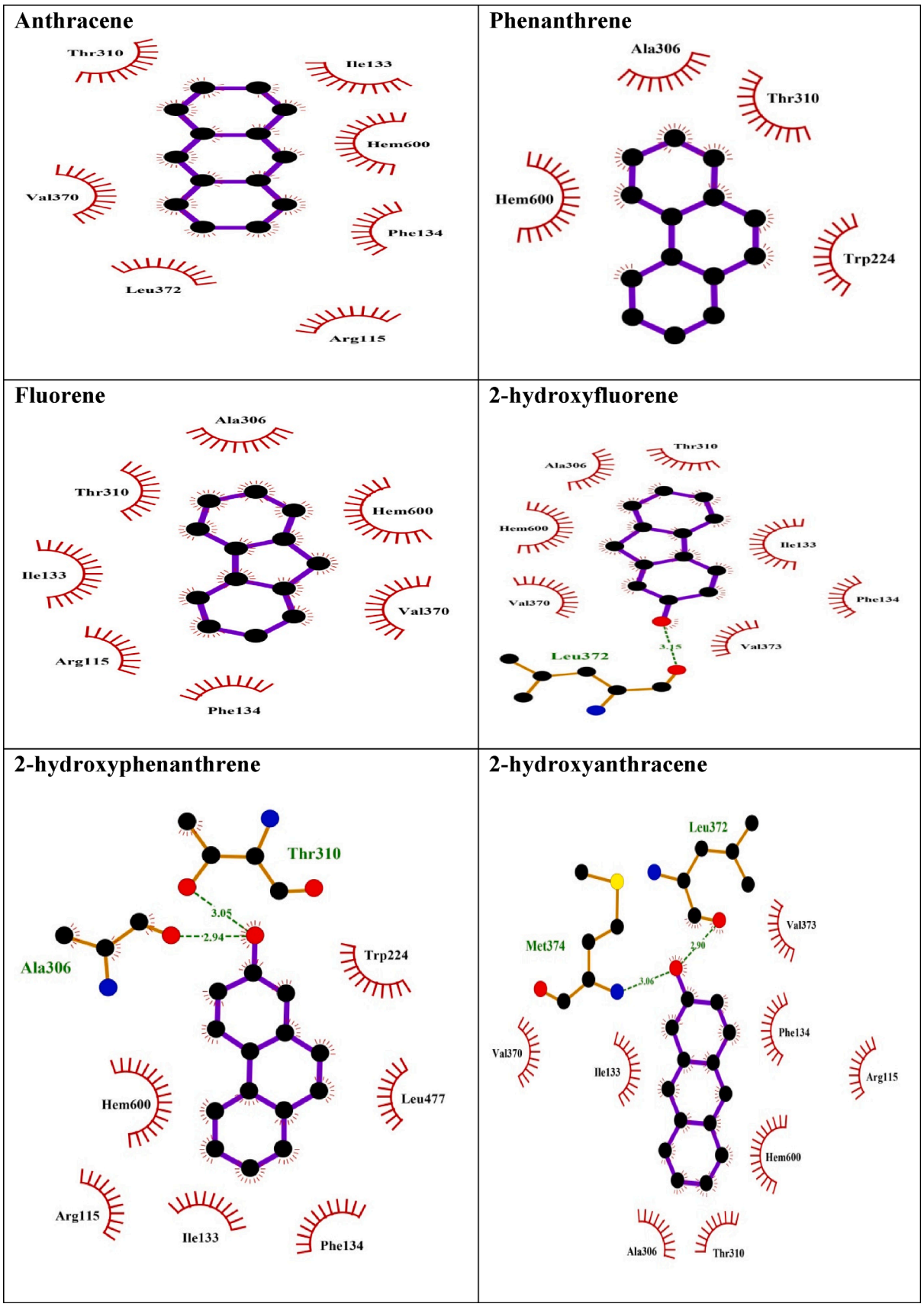

Fig. 4. (*continued*).

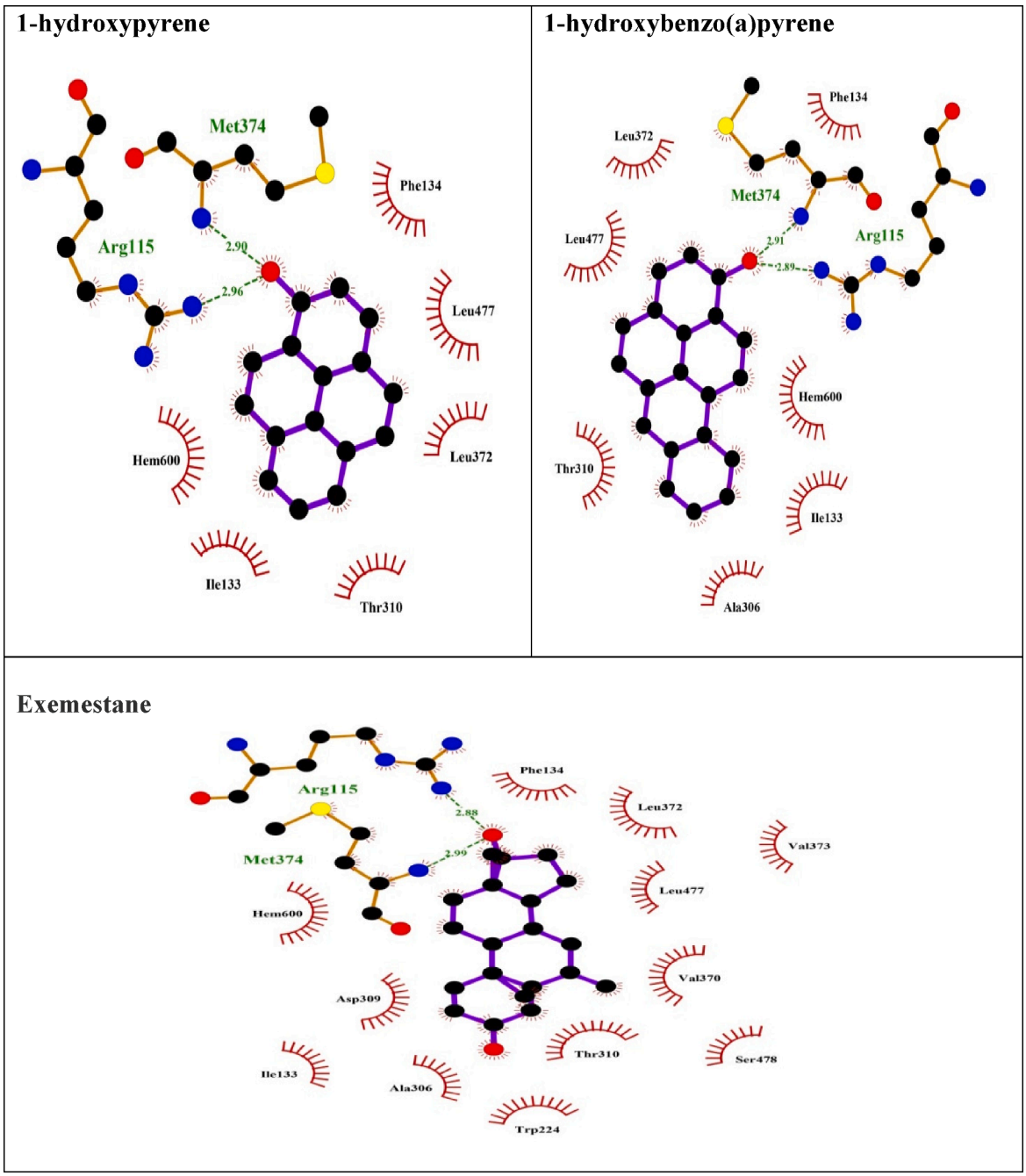

Fig. 4. (*continued*).

activity may lead to the elevation of androgen levels which is often associated with several disorders. PAHs and oxy-PAHs are the ubiquitous environmental compounds which have endocrine disruption and teratogenic properties. These toxicants have been investigated as inhibitors for aromatase by DFT and molecular docking calculations. This computational study shows that the PAHs-CYP19A1 complexes have binding affinities similar to known inhibitor-protein complex i.e. EXEMESTANE-CYP19A1. Hence, PAHs and their metabolites can efficiently bind to CYP19A1 and inhibit its activity in the steroid biosynthesis pathway. Our study emphasizes on the inhibitory effects of PAHs and oxy-PAHs on aromatase activity. It could be concluded that these parameters share together with different magnitudes and affect the degree of the binding affinity of these pollutants with the active protein sites to afford a certain degree of inhibition.

Declaration of Competing Interest

The authors declare that they have no known competing financial interests or personal relationships that could have appeared to influence the work reported in this paper.

Acknowledgement

The authors are thankful to Central Facility for Computational Research (CFCR), University of Lucknow for providing access to computational models throughout the work.

Funding

This research received no external funding.

References

[1] M.R. Yadav, M.A. Barmade, R.S. Tamboli, P.R. Murumkar, Developing aromatase inhibitors- an effective armament to win the battle against breast cancer, Eur. J. Med. Chem. 105 (2015) 1–38.

[2] Shabana,, et al., Potential utility of natural products as regulators of breast cancer-associated aromatase promoters, Reprod. Biol. Endocinol. 9 (2011) 91.

[3] S. Chen, Modulation of aromatase activity and expression by environmental chemicals, Fron. Biosci. 7 (2002) 1712–1719.

[4] Y.-C. Kao, K.R. Korzekwa, C.A. Laughton, S. Chen, Evaluation of the mechanism of aromatase cytochrome P450, Eur. J. Biochem. 268 (2001) 243–251.

[5] A.M. Vinggaard, C. Hnida, J.C. Larsen, Environmental polycyclic aromatic hydrocarbons affect androgen receptor activation in vitro, Toxicology 145 (2000) 173–183.

[6] Y. Lin, et al., Urinary metabolites of polycyclic aromatic hydrocarbons and the association with lipid peroxidation: A biomarker-based study between Los Angeles and Beijing, Environ. Sci. Technol. 50 (2016) 3738–3745.

[7] T.L. Smith, S.T. Merry, D.L. Harris, J.J. Ford, J. Ike, A.E. Archibong, et al., Species-specific testicular and hepatic microsomal metabolism of benzo(a)pyrene, an ubiquitous toxicant and endocrine disruptor, Toxicol. In Vitro 21 (2007) 753–758.

[8] Y. Zhang, et al., Biological impact of environmental polycyclic aromatic hydrocarbons (epahs) as endocrine disruptors, Environ. Pollut. 213 (2016) 809–824.

[9] C. Xu, et al., Ovotoxicity and PPAR-mediated aromatase downregulation in female Sprague-Dawley rats following combined oral exposure to benzo[a]pyrene and di-(2-ethylhexyl) phthalate, Toxicol. Lett. 199 (2010) 323–332.

[10] B.W.T. Ronny, A.T. Guay, W.J.G. Hellstrom, Clinical use of aromatase inhibitors in adult males, Sex. Med. Rev. 2 (2014) 79–90.

[11] D.I. Shulman, G.L. Francis, M.R. Palmert, E.A. Eugster, Use of aromatase inhibitors in children and adolescents with disorders of growth and adolescent development, Pediatrics 121 (2008) e975–e983.

[12] A. Le Maire, W. Bourguet, P. Balaguer, A structural view of nuclear hormone receptor: endocrine disruptor interactions, Cell. Mol. Life Sci. 67 (2010) 1219–1237.

[13] E. Stogiannidis, R., Laane, Source characterization of polycyclic aromatic hydrocarbons by using their molecular indices: an overview of possibilities, Rev. Environ. Contam. Toxicol. 234 (2015) 49–133.

[14] M.P. Gleeson, D. Gleeson, QM/MM calculations in drug discovery: A useful method for studying binding phenomena, J. Chem. Inform. Model. 49 (2009) 670–677.

[15] A.D. Becke, Density-functional exchange-energy approximation with correct asymptotic behavior, Phys. Rev. A 38 (1988) 3098–3100.

[16] C. Lee, W. Yang, R.G. Parr, Development of the Colle-Salvetti correlation-energy formula into a functional of the electron density, Phys Rev B 37 (1988) 785–789.

[17] Frisch MJ (2009) Guassian 09, Gaussian, Wallingford, CT, There is no corresponding record for this reference.

[18] H. Kruse, L. Goerigk, S. Grimme, Why the Standard B3LYP/6-31G* model chemistry should not be used in DFT calculations of molecular thermochemistry: understanding and correcting the problem, J. Org. Chem. 77 (2012) 10824–10834.

[19] G.M. Morris, R. Huey, W. Lindstrom, M.F. Sanner, R.K. Belew, D.S. Goodsell, A. J. Olson, autodock4 and autodocktools4. Automated docking with selective receptor flexibility, J. Comput. Chem. 30 (2009) 2785–2791.

[20] R. Dennington, T. Keith, J. Millam, Gaussview, version 5, Semichem Inc., Shawnee Mission, KS, USA, 2009.

[21] J.L. Calais, R.G. Parr, W. Yang, Density-functional theory of atoms and molecules, Int. J. Quantum Chem. 47 (1993) 101.

[22] R.G. Pearson, The HSAB Principle-more quantitative aspects, Inorg. Chim. Acta 240 (1995) 93–98.

[23] R.G. Pearson, Absolute electronegativity and hardness correlated with molecular orbital theory, Proc. Natl. Acad. Sci. 83 (1986) 8440–8441.